

Shadow charge detectability in large-scale neutrino detectors

N. Moller^{1*}, A. Obertacke¹

E-mail: nmoller1@icecube.wisc.edu

Very recent works predict the existence of a new type of "particle" that has rich phenomenology and carries profound implications for our understanding of the early universe. Furthermore, it could represent a fraction of the dark matter density. The so-called *shadow charges* leverage a fundamental principle: classical laws of physics are a mere limit of the deeper quantum mechanical laws. This simple argument has deep consequences, such as the existence of a "shadow" charge density that follows geodesics independently of any surrounding matter fields. We propose that this charged radiation can produce light when passing through a medium like the Earth, similarly to an infinitely massive ion. We provide an analytical study of their interactions in the South-Pole ice for direct application in the IceCube detector and trivial adaptation to any water-based experiment such as KM3NeT. Moreover, we present and discuss very first constraints on the shadow charge parameter space. Finally, we discuss the impact of a screening effect on their interaction with matter.

¹ *IceHap, Chiba University, Japan*

* Presenter

39th International Cosmic Ray Conference (ICRC2025)
15–24 July 2025
Geneva, Switzerland



1. Introduction

The central challenge in exotic particle searches lies less in the formulation of plausible theories than in their experimental testability. Recently, it was proposed that the initial state of the universe can be so that classical equations are violated as long as the quantum mechanical laws—the more correct laws of nature—are unbroken, and that relics of this initial state might still exist today [1]. We propose that these relics, the so-called *shadow charges*, can be observed in large scale light detectors such as neutrino observatories.

The framework for this theory is a relaxed version of quantum electromagnetism. In such a gauge theory, the number of physical degrees of freedom is smaller than the number of fields appearing in the classical action, and consequently fewer than the number of classical equations that can be derived from it. The physical fields lead to dynamical equations (second-order in time), while the non-physical fields lead to constraints on the physical ones. Gauss's law exemplifies such a constraint equation: it is a first-order, non-dynamical equation that arises from the gauge freedom inherent in the theory.

In the quantum formulation, however, there is only the Schrödinger equation, which dictates the time evolution of physical fields. As a result, in the classical limit of quantum electromagnetism, only the second-order, dynamical Maxwell equations are retained. To recover Gauss's law, one must additionally impose a specific choice of initial condition to the quantum theory: the state of lowest energy.

As no fundamental principle motivates this particular choice, the theory can be relaxed by not imposing any initial condition, resulting in the violation of Gauss's law: $\vec{\nabla} \cdot \vec{E} - j_0 \neq 0$. In the quantum formulation, this is equivalent to introducing a new current J_0^d :

$$\left(\vec{\nabla} \cdot \vec{E} - \hat{J}_0 \right) (\vec{x}) |\psi_{EM}\rangle = J_0^d(\vec{x}) |\psi_{EM}\rangle. \quad (1)$$

This additional term behaves like a fixed background charge density (no time evolution), and adds no microphysics to the theory as it simply reflects a choice of electromagnetic quantum state. Furthermore, it couples to gravity via the modified Maxwell equations:

$$\nabla_\mu F^{\mu\nu} = (J^\nu + J_{aux}^\nu) \quad (2)$$

$$J_{aux}^\mu = \frac{J_0^d(\vec{x})}{\sqrt{-g}} V^\mu. \quad (3)$$

From equation (3), it follows that the auxiliary current follows geodesic motion ($V^\mu \nabla_\mu V^\nu = 0$), and since it does not evolve, it can be interpreted as a static background charge density that does not respond to electromagnetic forces but remains gravitationally bound to large structures such as galaxies.

In a particle-like interpretation, one can consider the case where this background *shadow* charge density is peaked around point-like regions of space. These so-called *shadow charges* are thus not particles in the conventional sense, as they possess no mass. Rather, a shadow charge should be envisioned as a propagating electric field centered around a virtual charge—an entity defined by its field configuration rather than by intrinsic particle properties. Nonetheless, the particle-like picture leads to interesting phenomenology as it makes shadow charges behave like unstoppable

ions, allowing them to capture surrounding charged particles and therefore acquire a mass. This mass then allows shadow charges to contribute to the dark matter density observed in the universe.

We propose that shadow charges, when not fully screened by Standard Model particles, can interact with ordinary matter by exciting atomic electrons or displacing atomic nuclei, leading to isotropic light emission. As a result, shadow charges could produce detectable light signals while passing through the Earth, offering a potential observational signature in large-scale optical detectors such as IceCube [2], KM3NeT [3] or Baikal-GVD [4].

2. Interaction with Matter and Orbital Constraints

Shadow charges are strange objects in that they completely ignore surrounding matter fields, yet ordinary matter is affected by them. A shadow charge following a geodesic will pass through the Earth without suffering any loss of energy. However, atoms along its trajectory will interact with its electric field as if it were any charged Standard Model particle, gaining energy in the process. On a microscopic level, this results in an apparent violation of energy conservation, which must be reconciled by considering the macroscopic picture. The key idea is that the medium itself loses energy through "friction" as it moves through a cloud of charged matter, thereby balancing the microscopic energy gain with a macroscopic energy loss.

From the microscopic perspective, shadow charges can be modeled as infinitely massive ions traveling through the Earth at typical dark matter speeds ($\beta \sim 0.001$). In such a scenario, the interaction of the charged particle with atomic electrons is described by the following electronic energy loss formula [5]:

$$\left(\frac{dE}{dx}\right)_e = \frac{8\pi a_0 e^2 \beta}{\alpha} \frac{z_{SC}^{7/6} n_e}{(z_{SC}^{2/3} + Z^{2/3})^{3/2}} F(\beta) \quad (4)$$

where z_{SC} is the charge of the shadow charge, Z is the atomic number of the medium, n_e is its electronic density, a_0 is the Bohr radius, α is the fine-structure constant, $F(\beta) = 1 - \exp(-(\beta/\beta_0)^2)$ is a correction factor based on experimental data using slow protons [6], and $\beta_0 = 7 \times 10^{-4}$ is the fitted parameter. A slow charged particle can also interact with atomic nuclei by transferring kinetic energy to them. This is described by the nuclear energy loss formula [7]:

$$\left(\frac{dE}{dx}\right)_n = 4\pi a n_{nuc} z_{SC} Z e^2 S_n(\epsilon) \quad (5)$$

where n_{nuc} is the number density of nuclei, $a = 0.8853 a_0 \left(\sqrt{z_{nuc}} + \sqrt{Z}\right)^{-2/3}$ is the screening length and $S_n(\epsilon)$ is a function of the reduced energy ϵ defined in [7] and fitted on data. In the case of a shadow charge moving through a medium, these equations represent the internal energy gained by the medium as it traverses the electric field associated with a single shadow charge, per unit path length.

From the macroscopic point of view, the braking of the medium through interactions with shadow charges implies a net loss in the Earth's kinetic energy. Such a loss would affect the Earth's orbital parameters, in particular the semi-major axis. Since no deviation of this kind has been observed, the stability of the Earth's orbit can be used to place constraints on the amount of Earth's

kinetic energy converted into local excitation energy due to shadow charge interactions in the Earth. Fig. 1 shows the energy loss profile of a charged particle ($z_{SC} = 10$) passing through the Earth at a constant speed of $\beta = 10^{-3}$. The electron density profile used is taken from the PREM model [8] and the composition of the Earth is taken from [9].

We now make the following assumptions:

- Shadow charges all carry the same net charge, within the range $[1, 1/\alpha = 137]^1$, which remains constant during propagation.
- The Earth is spherical, its internal density follows the PREM model, and moves through a static cloud of shadow charges at a constant speed of $10^{-3}c$.
- 4.4 billion years ago, the Earth could not have been located further than 2.4 AU from the Sun; otherwise, the conditions required for liquid water would not have been met[11, 12].

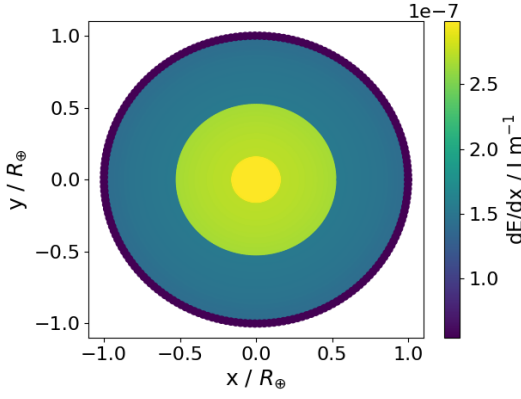


Figure 1: Energy loss profile of a charged particle ($z_{SC} = 10$) with constant speed ($\beta = 10^{-3}$) passing through the Earth (radius R_{\oplus}). The energy loss is computed using equations (4) and (5) and the PREM electron density profile [8].

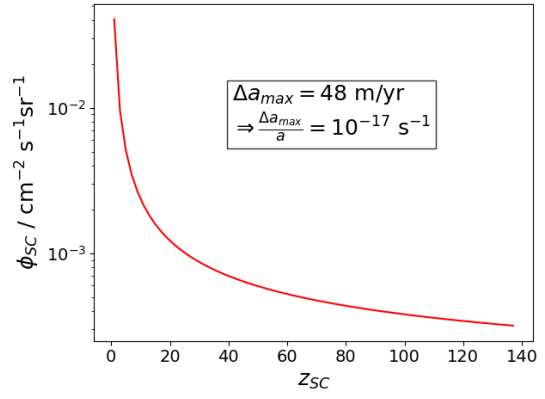


Figure 2: Upper flux limit of shadow charges, assuming a net charge in the range $z_{SC} \in [1, 137]$, based on their maximal allowed impact on the Earth–Sun distance.

To estimate the total orbital energy loss of the Earth over time, we integrate the energy loss from Fig. 1 along horizontal trajectories and initial y-axis entry points. This yields an expression for the Earth’s orbital energy loss rate as a function of the number of shadow charge and of their net charge $\dot{E}_{orb,\oplus}(n_{SC}, z_{SC})$. The Earth’s specific orbital energy is given by:

$$\mathcal{E}_{orb,\oplus} = \frac{E_{orb,\oplus}}{M_{\oplus}} = \frac{-\mu}{a} \quad (6)$$

where $\mu = GM_{\odot}$ is the standard gravitational parameter of the Sun and a is the semi-major axis of the Earth’s orbit. We then have the relation:

$$\frac{\dot{a}}{a_{today}} = \frac{a_{today} \dot{\mathcal{E}}_{orb,\oplus}}{\mu} = \frac{a_{today} \dot{E}_{orb,\oplus}(n_{SC}, z_{SC})}{\mu M_{\oplus}} \quad (7)$$

¹The charge is limited to $1/\alpha$ by the Schwinger limit [10], above which the electric field at the particle’s surface reaches m_e^2/e , leading to spontaneous pair production. The intrinsic charge, however, can be arbitrarily high, as it would simply emit pairs until it gets screened enough.

where $a_{\text{today}} = 1$ AU. Equation (7) links the stability of the Earth's orbit parameters to the number density of shadow charges n_{SC} and their net charge z_{SC} . Using the constraint from our last assumption—that the Earth could not have migrated inward more than 1.4 AU since the first trace of water—we obtain $\dot{a} < 48$ m/yr. This allows us to place an upper bound on the number density of shadow charges with a non-zero net charge (z_{SC}). The upper flux limit obtained from this calculation is shown in Fig. 2.

This flux limit is clearly ruled out by many orders of magnitudes by dark matter experiments such as MACRO [13], which obtained a flux limit of $2.6 \times 10^{-16} \text{ cm}^{-2} \text{ s}^{-1} \text{ sr}^{-1}$ for charged Q-balls by searching for energy deposits in their liquid scintillators [14]. Cosmology also constrains the net charge of shadow charges, as they would contribute to the radiation density in the early universe (Ω_R), which is tightly bounded by observations. A precise value is currently being determined.

3. Detectability

Luminescence refers to the emission of light by a substance that is not the result of thermal energy dissipation. It typically arises when a charged particle traverses a medium, exciting atoms along its path to higher excited states. As these atoms return to their ground state, they emit light isotropically. This process is a primary detection mechanism for charged particles that are too slow to ionize atoms in the medium or to produce Cherenkov radiation. Given the low velocities of shadow charges, luminescence is expected to represent their dominant detection channel, provided they carry a non-zero net charge.

The luminescence light yield depends on the energy loss of the particle and can be expressed as $\frac{dN}{dx} = S \cdot \frac{dE}{dx}$, where S is the scintillation efficiency, and is typically constant for small energy losses but decreases at higher values.

High-performance scintillators—such as plastic scintillators or thallium-doped sodium iodide (NaI(Tl))—are typically impurity-activated materials. These contain discrete, localized electronic levels between the valence and conduction bands, introduced by dopants (e.g., thallium in NaI), which facilitate efficient radiative transitions and light emission. In contrast, large-scale light detectors such as IceCube or Super-Kamiokande use extremely pure media like ice or water, which are intrinsically poor scintillators due to their minimal impurity content.

Experimental studies of ice and liquid water under irradiation at various temperatures measured light yields typically ranging from 1 to 10 photons per MeV of deposited energy [15] (see Fig. 3).

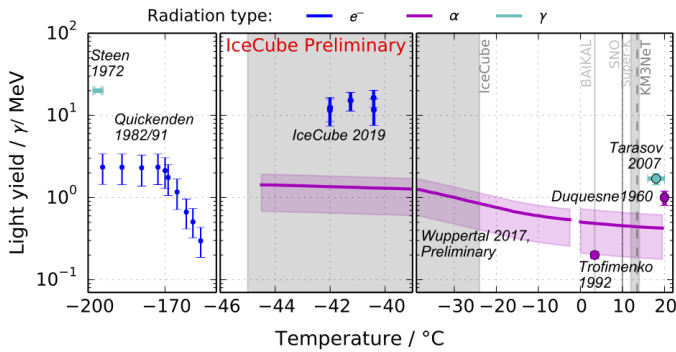


Figure 3: Scintillation response of pure ice and water to various types of radiations [15]. IceCube (2019) used a β -source in SPiceCore [16] (South Pole), while Wuppertal (2017) used an α -source in a laboratory setting. Shaded grey bands indicate the temperatures of common neutrino detectors.

In order to detect particles via luminescence in such pure media, the particle's energy loss must be sufficiently high. The energy loss of shadow charges, as given by equations (4) and (5), meets this requirement even for low values of the net charge (see Fig. 4). At high energy loss, however, the density of excited and ionized states becomes large enough for mutual interactions to occur. As a result, part of the deposited energy is dissipated thermally rather than being converted into light, a phenomenon known as *scintillation quenching*. This effect is often modeled through an intrinsic scintillation efficiency S_0 and a quenching parameter k , as in [17]:

$$\frac{dN}{dE} = \frac{S_0}{1 + k \left(\frac{dE}{dx} \right)_e}. \quad (8)$$

Using equation (7) and two data points from Fig. 3, we can find the values of S_0 and k that best fit the observed luminescence light in pure ice.

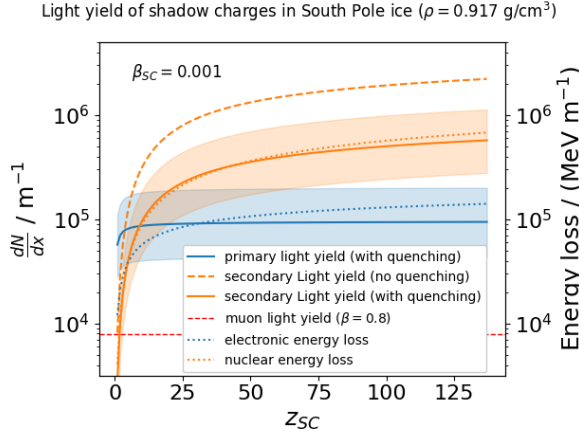


Figure 4: Energy loss and light yield of shadow charges ($\beta = 10^{-3}$) in pure ice ($\rho = 0.917 \text{ g/cm}^3$). The electronic and nuclear contributions are shown in blue and orange respectively. The uncertainty on the light yields comes from the ionization quenching parameters. For comparison, the red line shows the typical Cherenkov light yield of a muon detectable in IceCube.

The first data point is taken from the Wuppertal experiment, which measured an average of $N = (4 \pm 1.6)$ photons from $E_i = 4 \text{ MeV}$ α -particles [15]. As a second data point, we wish to take the value measured in SPICECore. However, the energy of the radiated electrons is still unclear and require further investigations. In the meantime, we use a value of k found in the literature² [17]: $k \sim (10 \pm 2) \text{ mg cm}^{-2} \text{ MeV}^{-1}$. We now solve the following equation for S_0 :

$$N = \int \frac{dN}{dx} dx = S_0 \int_0^{x_{\max}(E_i)} \frac{\left(\frac{dE}{dx} \right)_e}{1 + k \left(\frac{dE}{dx} \right)_e} dx \quad (9)$$

where x_{\max} is the stopping distance in ice and dE/dx is given by the Bethe-Bloch formula for electrons or α -particles. Using the Wuppertal measurement and the value of k from literature, equation (9) gives: $S_0 = 10_{-5}^{+8} \text{ MeV}^{-1}$. Using this result to calculate the light yield of shadow charges in the ice leads to the blue curve in Fig. 4. The total light yield of shadow charges is typically 1 to 2 orders of magnitude greater than that of a muon traveling at speed $\beta = 0.8$ (red dashed line), which is commonly detected in IceCube. This suggests that shadow charges should

²This value and its uncertainty are arbitrary approximations based on a set of experimental results ranging from ~ 9 to $\sim 11 \text{ mg cm}^{-2} \text{ MeV}^{-1}$, obtained with various organic scintillators.

be observable in IceCube-like experiments, provided that their signal can be distinguished from the increasing background associated with lower particle speeds (longer event duration).

As mentioned in the previous section, shadow charges can also transfer energy to atomic nuclei, which then produce luminescence light as well until they stop. The secondary light yield of shadow charges is then given by:

$$\left(\frac{dN}{dx}\right)_{nuc} = n_{nuc} \int_0^{T_m} L_p(T) \frac{d\sigma}{dT} dT \quad (10)$$

where $L_p(T)$ is the number of photons produced by a nucleus of initial kinetic energy T until it stops, σ is the nuclear cross section given in [18], and T_m is the maximum energy transferable to the nucleus. $L_p(T)$ is given by:

$$L_p(T) = \int_0^E \frac{\frac{dN}{dx}(\epsilon)}{\left(\frac{dE}{dx}\right)_{tot}} d\epsilon \quad (11)$$

where $\frac{dN}{dx}$ is the quenched luminescence yield given by the product of equation (8) and equation (4), and $\left(\frac{dE}{dx}\right)_{tot}$ is the sum of equations (4) and (5).

4. Bound States

During the period of recombination, where electrons started forming bound states with protons, they could just as well recombine with positive shadow charges. Not only electrons, but any charged particle existing in the early universe could have recombined with a shadow charge of opposite charge, except unstable particles such as the *top*-quark which are very likely to decay before forming any bound state. Bound states made of anti-matter particles are also not expected today as their binding energy is typically way below the temperature at which they decouple from the thermic bath and start annihilating with normal matter. As a first assumption, we thus only expect shadow bound systems made of protons or electrons bound to respectively negative shadow charges (NSC) or positive shadow charges (PSC). Since protons (due to their higher mass) decouple from the thermic bath earlier than electrons, NSCs would be screened earlier than PSCs.

The period of recombination is followed by a period of reionization, where radiation from the very first stars strips atoms from their electrons. We thus expect shadow bound systems to be at least partially re-ionized during this period, the effect being stronger on PSCs than NSCs as the binding energy of protons is $m_p/m_e \sim 1000$ times higher than the one of electrons. Today, we thus expect PSCs with a non-zero effective charge to cross the Earth and produce luminous signals, while NSCs could remain screened and are thus less likely to be detectable.

5. Discussion and Outlook

Shadow charges are relics of the early universe that could, for the first time, provide an avenue to probe its initial state. If not diluted by a period of inflation, they may still exist today, potentially contributing to the observed dark matter density, and produce luminous signals while traversing the Earth. They open up rich new phenomenology, some of which is still under investigation. For instance, a full treatment of their propagation—accounting for electron/proton capture and ionization—is still lacking. It is also not forbidden that NSCs bind to heavier nuclei. Moreover,

shadow charges could possess non-integer values. Finally, interactions with the Higgs boson before electroweak decoupling might have shaped shadow bound systems in a very unique way.

Acknowledgements: The authors are grateful to Tom Melia, Surjeet Rajendran and Francesco Serra for their insightful discussions and valuable input regarding the phenomenology of shadow charges.

References

- [1] D. E. Kaplan, T. Melia, S. Rajendran, L. D. Grosso, V. Poulin, and T. L. Smith, “The classical equations of motion of quantized gauge theories, parts i & ii; cosmological consequences of unconstrained gravity and electromagnetism,” 2023–2024. [arXiv:2305.01798](#), [arXiv:2307.09475](#), [arXiv:2405.06374](#).
- [2] **IceCube** Collaboration, M. G. Aartsen *et al.* *JINST* **12** (2017) P03012.
- [3] **KM3NeT** Collaboration, S. Adrián-Martínez *et al.* *J. Phys. G* **43** (2016) 084001.
- [4] A. D. Avrorin *et al.* *EPJ Web Conf.* **207** (2019) 06001.
- [5] J. Lindhard and M. Scharff *Phys. Rev.* **124** (Oct, 1961) 128–130.
- [6] D. J. Ficenec, S. P. Ahlen, A. A. Marin, J. A. Musser, and G. Tarlé *Phys. Rev. D* **36** (Jul, 1987) 311–314.
- [7] W. D. Wilson, L. G. Haggmark, and J. P. Biersack *Physical Review B* **15** no. 5, (Mar., 1977) 2458–2468.
- [8] A. M. Dziewonski and D. L. Anderson *Physics of the Earth and Planetary Interiors* **25** no. 4, (1981) 297–356.
- [9] F. D. Stacey and P. M. Davis, *Physics of the Earth*. Cambridge University Press, Cambridge, UK, 4th ed., 2008.
- [10] J. Schwinger *Phys. Rev.* **82** (Jun, 1951) 664–679.
- [11] “Origin of water on earth.” <https://courses.seas.harvard.edu/climate/eli/Courses/EPS281r/Sources/Origin-of-oceans/1-Wikipedia-Origin-of-water-on-Earth.pdf>, 2020. Accessed from Harvard University course material.
- [12] R. M. Ramirez and L. Kaltenegger *The Astrophysical Journal Letters* **837** no. 1, (Feb., 2017) L4.
- [13] I. D. Mitri *arXiv preprint hep-ex/0212055* (2002) .
- [14] I. De Mitri *Nuclear Physics B - Proceedings Supplements* **110** (July, 2002) 186–188.
- [15] A. Pollmann *PoS ICRC2021* (2021) 1093.
- [16] K. Casey, T. Fudge, T. Neumann, E. Steig, M. Cavitte, and D. Blankenship *Annals of Glaciology* **55** no. 68, (2014) 137–146.
- [17] J. B. Birks, *The Theory and Practice of Scintillation Counting*. Pergamon Press, Oxford, 1964.
- [18] J. Lindhard, M. Scharff, and H. E. Schiøtt *Kongelige Danske Videnskabernes Selskab, Matematisk-Fysiske Meddelelser* **33** no. 14, (1963) 1–42.